JOURNAL OF BACTERIOLOGY, June 1996, p. 3654–3657 Vol. 178, No. 12
0021-9193/96/$04.00+0

Differential Domain Accessibility to Monoclonal Antibodies in Three Different Morphological Assemblies Built Up by the S-Layer Protein of *Thermus thermophilus* HB8

JOSÉ R. CASTÓN,[1]† GARBIÑE OLABARRÍA,[1] IÑIGO LASA,[1]‡ JOSÉ L. CARRASCOSA,[2] AND JOSÉ BERENGUER[1]*

Centro de Biología Molecular "Severo Ochoa"[1] and Centro Nacional de Biotecnología,[2] Universidad Autónoma de Madrid, 28049 Madrid, Spain

Received 16 January 1996/Accepted 1 April 1996

A collection of 27 monoclonal antibodies (MAbs) against the S-layer protein (P100) of *Thermus thermophilus* HB8 has been obtained. They have been classified according to their ability to recognize S-layer regions expressed in *E. coli* from plasmids containing different fragments of its coding gene, *slpA*. The accessibility of the binding sites in hexagonal, trigonal, or tetragonal assemblies of P100 was analyzed by enzyme-linked immunosorbent assays with six of these MAbs and their respective Fab fragments. When packed hexagonally as the native S-layer (S1 assemblies), only a small region located near the amino terminus of the P100 was accessible. However, when P100 was assembled into trigonal (pS2 assemblies) or tetragonal (S2 assemblies) arrays, most of the protein domains analyzed were easily detected, thus suggesting that P100 is assembled in S2 and pS2 in a similar way and that these two arrangements are quite different from the S1 assembly. Relationships between accessibility and sequence predictions are discussed.

Thermus thermophilus HB8 is a thermophilic eubacterium that belongs to one of the oldest phylogenetic groups of the domain *Bacteria* (9). As its outermost layer, this organism has an hexagonal array whose building block, a 100-kDa protein called P100, has been extensively studied (5–7). The P100 protein has the exceptional ability to form assemblies in vitro with three different symmetries: hexagonal, trigonal, and tetragonal (3).

The hexagonal arrangements of P100, called S1 assemblies, are indistinguishable from the paracrystalline S-layer found in the cells and require for their structural integrity the presence of peptidoglycan as a component of the structure (3). Thin sections revealed that S1 crystals are a double protein layer of hexagonally packed P100 proteins in which the central massive regions, which correspond to the P6 symmetry axis, interact in a perfect register (3). Subsequent three-dimensional analysis (2) revealed that these hexagonal centers were connected in each layer through double arms at trigonal (P3) centers near the external surface of the structure.

Analysis of the tetragonal arrays of P100, called S2 assemblies, revealed a completely different architecture. These are single layers of protein in which the structural units appear as trimers of P100. The mass distribution of these assemblies was similar in general architecture to that built up by gram-negative porins (4, 17), a feature that may support the proposed common origin for both S-layers and porins (12).

While for S1 and S2 assemblies of P100 the presence of additional cell envelope components (see above) is required, purified P100 protein assembles into trigonal (pS2) arrays (3). The analysis of this trigonal structure revealed an architecture that resembled that of an intermediate structure between the hexagonal (S1) and tetragonal (S2) assemblies. Supporting this view were the findings that pS2 could be obtained from S1 assemblies by detergent (Triton X-100) treatment after digestion of the peptidoglycan layer, and that, conversely, S2 could be transformed to pS2 assemblies through EDTA-Triton X-100 treatments.

The structural transformations of P100 assemblies described above were observed in situ as a consequence of a rearrangement process that does not require any step of subunit dissociation (3). Thus, such transformations must rely on the persistence of some of the essential interactions during the rearrangement process. In this sense, the single common motif found for all three assemblies was the presence of trigonal interactions that was correlated with the presence of calcium-dependent P100 trimers, which are strong enough to withstand even boiling in 10% sodium dodecyl sulfate solutions (3, 5).

In order to analyze which domains of the P100 protein were implicated in the rearrangement of the protein to accommodate the shift from the native hexagonal structure to the trigonal and tetragonal assemblies, we produced a number of monoclonal antibodies against different P100 regions. In this article we describe the characterization of monoclonal antibodies (MAbs) against P100 and their accessibility to the corresponding epitopes in each of its three possible regular assemblies.

MAbs against P100. To obtain antibody-producing hybridomas, 8-week-old BALB/c mice were immunized by standard procedures with P100 protein purified from sodium dodecyl sulfate-polyacrylamide gels (SDS-PAGE) (1). Spleen cells were subsequently fused to mouse myeloma X63/Ag 8.653 cells as previously described (13, 16). Fusions were analyzed through radioimmunoassays (8, 16) by using P100 protein purified from gels as antigens.

A total of 27 hybridomas were selected because their culture supernatants strongly recognized the P100 protein. Once cloned and expanded, BALB/c mice were used to obtain the corresponding ascitic fluids with high MAb concentration.

* Corresponding author. Phone: 34-1-3978099. Fax: 34-1-3978344. Electronic mail address: JBERENGUER@mvax.cbm.uam.es.

† Present address: Building 6, Laboratory of Structural Biology, National Institutes of Health, Bethesda, MD 20892.

‡ Present address: Departamento de Producción Agraria, E.T.S. Ingenieros Agrónomos, Universidad Pública de Navarra, 31006-Navarra, Spain.

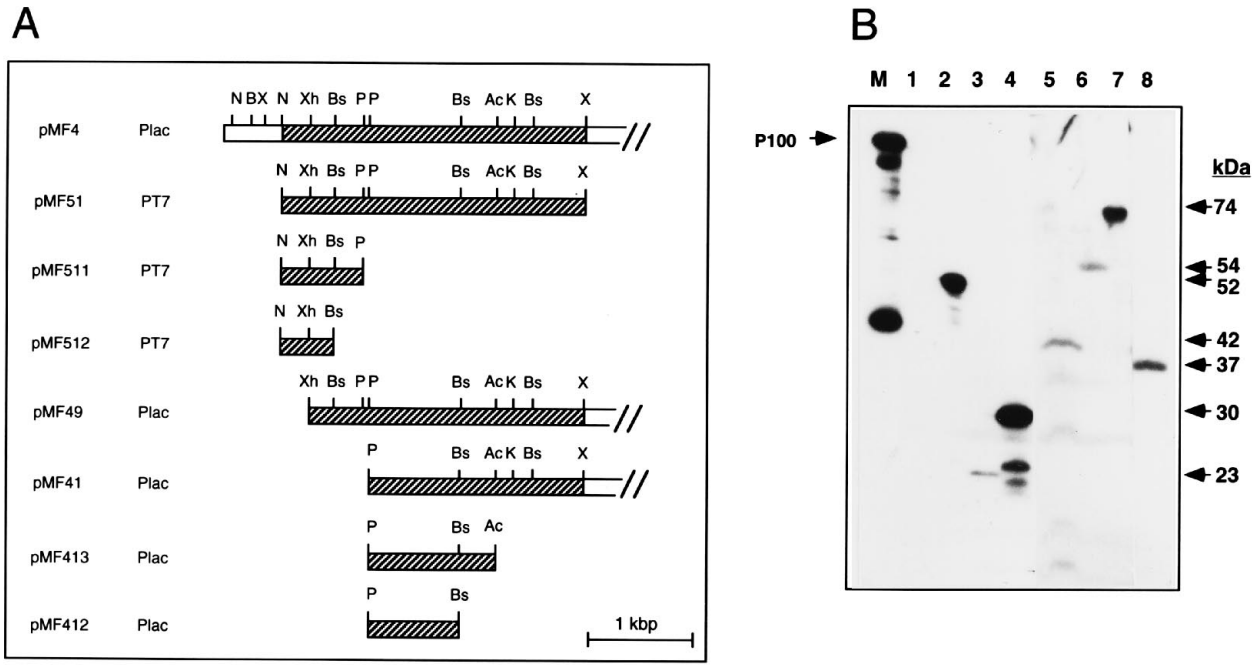

FIG. 1. Expression in *E. coli* of different *slpA* regions. (A) Plasmids and promoters used for the expression of *slpA* fragments in *E. coli* are shown at left. Coding regions for *slpA* are hatched. Restriction enzymes: Ac, *Acc*I; B, *Bam*HI; Bs, *Bst*EII; K, *Kpn*I; N, *Nde*I; P, *Pst*I; X, *Xma*I; and Xh, *Xho*I. (B) Plasmids pMF51 (lane 2), pMF512 (lane 3), pMF511 (lane 4), pMF412 (lane 5), pMF413 (lane 6), pMF41 (lane 7), and pMF49 (lane 8) were expressed at 37°C for 6 h in the presence of isopropyl-β-D-thiogalactopyranoside (2 mM) in *E. coli* strain BL21DE3 (pMF5. . . series) or JM109 (pMF4. . . series), and specific P100 fragments were subsequently detected with polyclonal rabbit α-P100 antiserum by Western blotting of total protein extracts. Samples in lanes M and 1 correspond to membrane proteins from *T. thermophilus* HB8 and from a cell extract of *E. coli* JM109, respectively. The sizes (in kilodaltons) of the expressed P100 fragments are shown at right.

The molecular characterization of the MAbs demonstrated that most of them belonged to the G1 (18 MAbs) and G2b (3 MAbs) isotypes. The other six MAbs belonged to the M isotype. Unfortunately, two of these MAbs (2AD10 and 3EE12) were the only ones that recognized the carboxylic end of the protein, a fact that made their use in enzyme-linked immunosorbent assays (ELISA) extremely difficult (see below).

Expression of different P100 fragments in *Escherichia coli*. To identify which regions of the P100 protein were recognized by the MAbs, we expressed plasmids containing different regions of the P100 encoding gene (*slpA*) in *E. coli* (7). The expression products were further used in Western blot (immunoblot) experiments to localize P100 regions specifically identified by the MAbs (from ascitic fluid).

Figure 1A shows the plasmids used for this identification, along with the promoters used for their expression in *E. coli*. As shown in Table 1, all but plasmids pMF51 (6) and pMF49 caused expression of a protein band whose electrophoretical mobility corresponded to the size expected from their respective constructions.

TABLE 1. Expected sizes and observed electrophoretic mobilities of the products expressed in *E. coli* from different plasmids

Plasmid	Size (in kDa) of expected product	Observed mobility (kDa)
pMF51	100	52
pMF511	27.9	30
pMF512	21.8	23
pMF49	89.5	37
pMF41	71	74
pMF413	47.2	54
pMF412	31	42

Plasmids pMF51 (6), pMF511, and pMF512 are derivatives from pAR3038 (15) in which regions corresponding to the amino terminus of *slpA* were expressed from a T7 promoter. The expression by pMF51 of a 52-kDa protein (Fig. 1B, lane 2) instead of the full-size P100 protein (Table 1) was previously demonstrated to be due to the proteolytic processing of the corresponding expression product in *lon*$^+$ cells (6). Since the amino-terminal sequencing of the fragment expressed by pMF51 revealed that it started at the first ATG codon of *slpA*, a positive identification by an MAb allowed us to localize the corresponding epitope at the first half of the protein.

Plasmids pMF49, pMF41, pMF413, and pMF412 are derivatives of pMF4 (6) and pUC9 (19) from which the *slpA* fragments shown in Fig. 1A were expressed from the pLac promoter. As noted before (Table 1), all but pMF49 caused expression of a protein band that was recognized by α-P100 polyclonal antiserum and whose mobility corresponded to that expected from the sequence. The expression of a 37-kDa protein from cells carrying plasmid pMF49 (Fig. 1B, lane 5), instead of the expected 89-kDa protein could probably be related to the same effect observed for pMF51 (Fig. 1B, lane 2).

Identification of P100 domains recognized by the MAbs. The first step in the identification of the region recognized by the MAbs was to separate them on the basis of which of them recognized the product of pMF511 (amino acids 1 to 261) and which of them recognized the product of pMF41 (amino acids 288 to 917). MAbs specific for the amino terminus were subsequently selected for their ability to recognize the product of pMF512 (amino acids 1 to 196). MAbs resulting from this selection were then assayed for their ability to recognize the product of pMF49 (starting at amino acid position 98).

A similar approach was followed to classify the MAbs which recognized the products of pMF41. Those that did not recognize the product of pMF413 should be directed against an

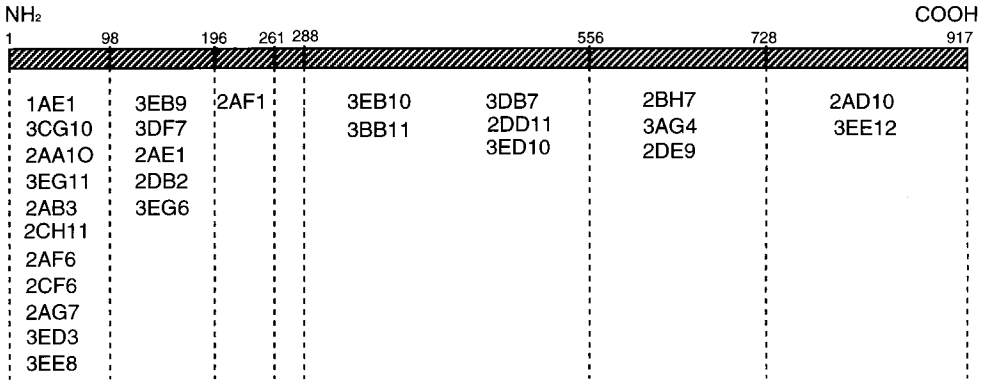

FIG. 2. Distribution of MAbs by their specificity along the P100 sequence. Each MAb was assayed by Western blot experiments to identify the different P100 fragments expressed (see Fig. 1). The name of each MAb is shown below the P100 region that contains the corresponding epitope.

epitope located between positions 728 and 917, and those that recognized the expression product of pMF413 and not the one from pMF412 were specific for the differential region (positions 556 to 728). Finally, those which recognized the product of pMF412 (positions 288 to 556) were divided by their ability to recognize or not the products of pMF51, which ends at the middle of the protein.

The classification of MAbs through the process described above is shown in Fig. 2. Of 27 MAbs analyzed, 11 recognized the product of pMF512 but not the product of pMF49 and therefore were specific for an apparently highly immunogenic region located in the first 98 amino acids of P100 (from the starting ATG to the *Xho*I site). Computer analysis of this region predicts the existence of a sequence (amino acids 77 to 89) with an antigenicity index (AI) higher than 0.9 according to the system of Jameson and Wolf (10). Another important group of MAbs was found to recognize a region between amino acids 98 and 196, where computer predictions suggest the existence of a highly immunogenic region (positions 109 to 116). An average of two to three MAbs was identified for each of the remaining regions of the P100 sequence, except for the region between amino acids 196 and 261 (*Bst*EII-*Pst*I region of P100), which was recognized only by MAb 2AF1.

Accessibility of P100 regions in S1, S2, and pS2 assemblies. In order to analyze the accessibility of different P100 regions in S1, S2, and pS2 assemblies, a high affinity MAb belonging to the G1 isotype was selected for each of the regions studied. The MAbs selected, 1AE1, 3EB9, 2AF1, 3EB10, 2DD11, and 2BH7, were purified from ascitic fluid (8) and their respective Fab fragments were obtained and separated by affinity chromatography as described previously (14).

The amount of complete MAbs and Fab fragments bound (after 18 h of incubation at room temperature) to 200 ng of P100 protein assembled in hexagonal (S1), trigonal (pS2), or tetragonal (S2) arrays (as verified by electron microscopy) was quantified through ELISA. The three different assemblies were obtained from purified cell envelopes of *Thermus thermophilus* HB8 as previously described (3).

The score results of at least 10 of these ELISAs are presented in Fig. 3. In this figure, the percentage of the adsorption values with respect to a rabbit polyclonal antiserum α-P100 (6) were represented for each of the three P100 assemblies. As a negative control we used the values obtained with a purified ribosomal protein (200 ng) with the same α-P100 polyclonal antiserum.

As may be observed, most of the P100 regions remained undetected when packed in hexagonal arrangements (S1), with the exception of the epitope recognized by MAb 3EB9 (positions 98 to 196). Similar data were obtained with the respective Fab fragments.

By contrast, in S2 and pS2 assemblies most of the P100 domains were detected with the MAbs thus showing that the transition from hexagonal (S1) to trigonal (pS2) or tetragonal

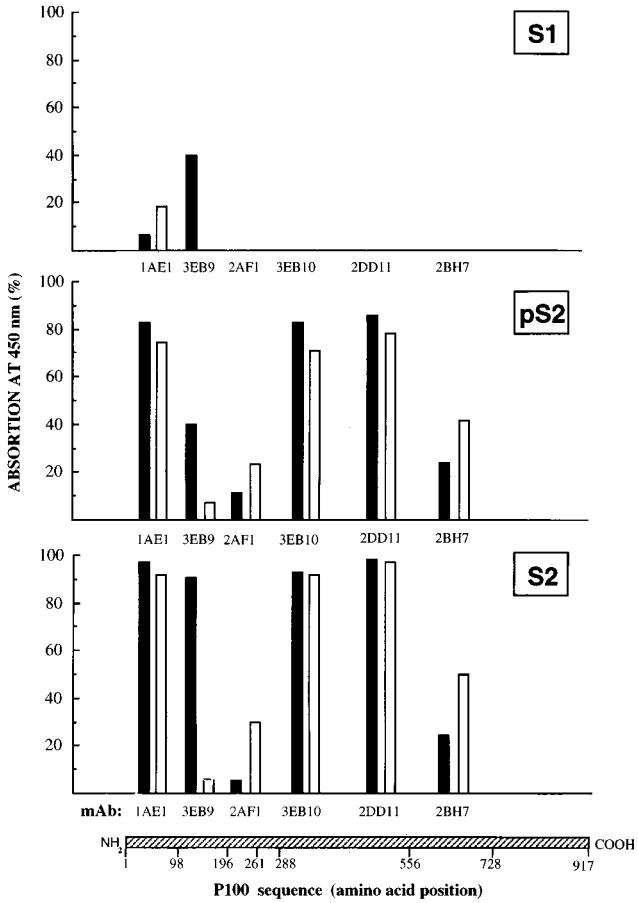

FIG. 3. Accessibility of MAbs and the corresponding Fab fragments to different P100 regions. The percentage of recognition for each of the MAb (black bars) indicated and for its Fab fragment (white bars) are given relative to the value obtained with a polyclonal rabbit antiserum in ELISAs for the hexagonal (S1), trigonal (pS2), and tetragonal (S2) assemblies of the P100 protein.

(S2) arrays implies the movement to the surface of protein domains that were formerly inaccessible. This is especially relevant for MAbs 1AE1, which recognizes a region in the amino terminus of the protein, and 3EB10, 2DD11, and 2BH7, which recognize regions between positions 288 and 728.

The differences in accessibility described above pose the question of whether these differences are due to an intramolecular rearrangement of protein domains or whether they are the consequence of the different quaternary assembly of the P100 monomers. As no high-resolution structural model of the monomers is available, we suggest that the epitopes recognized by these MAbs are located in an inner part of the S1 structure, whereas they are located at the surface in S2 and pS2 crystals. In addition, such differences in accessibility between S1 and S2/pS2 could be also explained by taking into account the bilayer nature of the S1 structure, with the same surface being exposed on both sides and most of the protein mass remaining undetected in the internal massive P6 centers. By contrast, the monolayer nature of S2 and pS2, as well as the lack of the massive hexameric centers, implies a higher surface/protein ratio and, in consequence, a more extended conformation of the P100 protein.

Especially relevant are the data obtained with MAb 1AE1. The region including the epitope recognized by this MAb has been proposed to contain a peptidoglycan-binding motif (11). The presence of such a motif is in good agreement with the observed requirements for peptidoglycan to preserve the S1 assembly (3). Thus, if such a motif were responsible for the peptidoglycan binding in the S-layer (indistinguishable from S1 assembly), it follows that this region should have an internal location in S1 crystals. The low accessibility to this region of MAb 1AE1 is in good agreement with this hypothetical location. In addition, it makes sense that degradation of peptidoglycan, required for the conversion of S1 to pS2, allows this domain to be exposed on the surface, leading to a dramatic increase in its accessibility (Fig. 3).

A partial reaction of S1 crystals could be achieved only with MAb 3EB9, thus suggesting that at least part of the region between amino acid positions 98 and 196 is located near the surface of the crystal, but not as exposed as it is in S2 arrangements. With pS2, a detection level similar to that of S1 was obtained, thus supporting the proposed intermediate nature of this structure. However, the decrease in the detection level with the corresponding Fab fragment remains unexplained.

There is a region between amino acids 196 and 261, recognized by MAb 2AF1, that remains poorly detected in all three of the arrangements studied. This implies that this region remains protected and suggests that it maintains a similar conformation in all three arrangements. A computer analysis of the sequence of this region predicts the presence of a strong calcium-binding site (positions 202 to 220) (7, 18) which could be responsible for the trimeric interaction detected as the single common structural and biochemical motif in the three arrangements of P100 (3).

The data presented in this paper show that only small regions of the P100 protein are exposed to the surface in the S-layer (identical to S1 crystals) of *T. thermophilus* and that the previously described structural transformations to trigonal and tetragonal arrangements imply an extreme reorganization which leads to an increase of the accessibility to MAbs along the whole polypeptide sequence. Whether this change in the accessibility of the different epitopes is due to an intermonomeric rearrangement of the protein or to a different quaternary structure of the protein remains unresolved until a more detailed model of the P100 subunit structure can be obtained. In addition, the data presented in this work are compatible with the existence of a peptidoglycan-binding domain at the amino terminus of the P100 protein and of a putative calcium-binding domain (positions 202 to 220). The binding of calcium by this domain seems to be the most important, if not the only interaction that remains stable through all three structural arrangements of the S-layer protein of *T. thermophilus* HB8.

We thank L. Enjuanes and C. Suñé for their advice on obtaining MAbs. The technical assistance of C. San Martín and J. de la Rosa is greatly appreciated.

This work has been supported by project numbers BIO94-0789 and PB91-0109 from the CICYT and by an institutional grant from Fundación Ramón Areces. J. R. Castón and I. Lasa are holders of fellowships from MEC, and G. Olabarría is a holder of a fellowship from Gobierno Vasco.

REFERENCES

1. **Boulard, C., and A. Lecroisey.** 1982. Specific antisera produced by direct immunization with slices of polyacrylamide gel containing small amounts of proteins. J. Immunol. Methods. **50:**221–226.
2. **Castón, J. R., J. Berenguer, E. Kocsics, and J. L. Carrascosa.** 1994. Three-dimensional structure of different aggregates built up by the S-layer protein of *Thermus thermophilus*. J. Struct. Biol. **113:**164–176.
3. **Castón, J. R., J. Berenguer, M. A. d. Pedro, and J. L. Carrascosa.** 1993. The S-layer protein from *Thermus thermophilus* HB8 assembles into porin-like structures. Mol. Microbiol. **9:**65–75.
4. **Dorset, D. L., A. Engel, M. Häner, A. Massalski, and J. P. Rosenbusch.** 1983. Two-dimensional crystal packing of matrix porin. A channel forming protein in *Escherichia coli* outer membranes. J. Mol. Biol. **165:**701–710.
5. **Faraldo, M. L., M. A. de Pedro, and J. Berenguer.** 1988. Purification, composition and Ca^{2+}-binding properties of the monomeric protein of the S-layer of *Thermus thermophilus*. FEBS Lett. **235:**117–121.
6. **Faraldo, M. L. M., M. A. de Pedro, and J. Berenguer.** 1991. Cloning and expression in *Escherichia coli* of the structural gene coding for the monomeric protein of the S-layer of *Thermus thermophilus* HB8. J. Bacteriol. **173:**5346–5351.
7. **Faraldo, M. M., M. A. de Pedro, and J. Berenguer.** 1992. Sequence of the S-layer gene of *Thermus thermophilus* HB8 and functionality of its promoter in *Escherichia coli*. J. Bacteriol. **174:**7458–7462.
8. **Harlow, E., and D. Lane.** 1988. Antibodies. A laboratory manual. Cold Spring Harbor Laboratory, Cold Spring Harbor, New York.
9. **Hartmann, R. K., B. Wolters, B. Kroger, S. Shultze, T. Spetch, and V. A. Erdmann.** 1989. Does *Thermus* represent another deep eubacterial branching? Syst. Appl. Microbiol. **11:**243–249.
10. **Jameson, B. A., and H. Wolf.** 1988. The antigenicity index: a novel algorithm for predicting antigenic determinants. Comput. Appl. Biosci. **4:**181–186.
11. **Lupas, A., H. Engelhardt, J. Peters, U. Santarius, S. Volker, and W. Baumeister.** 1994. Domain structure of the *Acetogenium kivui* surface layer revealed by electron crystallography and sequence analysis. J. Bacteriol. **176:**1224–1233.
12. **Messner, P., and U. B. Sleytr.** 1992. Crystalline bacterial surface layers. Adv. Microbiol. Physiol. **33:**213–275.
13. **Nowinski, R. C., M. E. Lostrom, M. R. Tam, M. R. Stone, and W. N. Burnette.** 1979. The isolation of hybrid cell lines producing monoclonal antibodies against the p15(E) protein of murine leukemia viruses. Virology **93:**111–126.
14. **Parham, P.** 1986. Preparation and purification of active fragments from mouse monoclonal antibodies, p. 14.1–14.22. *In* D. M. Weir (ed.), Handbook of experimental immunology. Blackwell Scientific Publications, Oxford.
15. **Rosenberg, A. H., B. N. Lada, D. Chui, S.-W. Lin, J. J. Dunn, and W. Studier.** 1987. Vectors for selective expression of cloned DNAs by T7 RNA polymerase. Gene **56:**125–135.
16. **Sanz, A., B. García-Barreno, M. L. Nogal, E. Viñuela, and L. Enjuanes.** 1985. Monoclonal antibodies specific for African swine fever virus proteins. J. Virol. **54:**199–206.
17. **Steven, A. C., B. Heggeler, R. Müller, J. Kistler, and J. P. Rosenbuch.** 1977. Ultrastructure of a periodic protein layer in the outer membrane of *Escherichia coli*. J. Cell. Biol. **72:**292–301.
18. **Valencia-Herrera, A., L. Menéndez-Arias, and L. Serrano.** 1988. La estructura tridimensional de las proteínas y los métodos de predicción a partir de la secuencia de aminoácidos: bases teóricas para el diseño. An. Quim. **84:** 223–266.
19. **Viera, J., and J. Messing.** 1982. The pUC plasmids, an M13mp7-derived system for insertion mutagenesis and sequencing with synthetic universal primers. Gene **19:**259–268.